ELSEVIER

Computational Materials Science 21 (2001) 69–78

COMPUTATIONAL MATERIALS SCIENCE

www.elsevier.com/locate/commatsci

A hybrid model for mesoscopic simulation of recrystallization

A.D. Rollett [a,*], D. Raabe [b]

[a] *Department of Materials Science and Engineering, Wean Hall 4315, Carnegie Mellon University, 5000 Forbes Avenue, Pittsburgh, PA 15213-2890, USA*

[b] *Max-Planck-Institut für Eisenforschung Max-Planck-Str. 1, 40237 Duesseldorf, Germany*

Received 17 November 1999; received in revised form 24 August 2000; accepted 10 October 2000

Abstract

A brief summary of simulation techniques for recrystallization is given. The limitations of the Potts model and the cellular automaton model as used in their standard forms for grain growth and recrystallization are noted. A new approach based on a hybrid of the Potts model (MC) and the cellular automaton (CA) model is proposed in order to obtain the desired limiting behavior for both curvature-driven and stored energy-driven grain boundary migration.

Keywords: Recrystallization; Modeling; Simulation; Monte Carlo; Potts model; Cellular automaton

1. Introduction

This paper gives a brief summary of mesoscopic methods for simulation of recrystallization and introduces a new approach for modeling the effects curvature-driven and stored energy-driven migration of boundaries. The standard form of the Monte Carlo (MC) model does not result in a linear relationship between migration rate and stored energy. On the other hand, the standard form of the cellular automaton (CA) model used for recrystallization does not allow for curvature as a driving force for migration. The basis for the new approach is the use of two different methods for determining orientation changes at each site in a lattice. The choice of which method to apply at any point in time is governed by weighting the probabilities for each type or reorientation attempt according to the desired balance in driving forces.

2. Summary of simulation methods

The need for computer simulation of recrystallization is driven by two different considerations. One is the need to be able to make quantitative predictions of the microstructure and properties of materials as affected by annealing. Simulation can be used to predict the average texture and grain size which strongly affect mechanical behavior. An equally important motivation for simulation, however, is the need for improved understanding of the recrystallization phenomenon that is highly complex from a microstructural point of view. The development of strong cube textures in fcc metals or the Goss texture in silicon steels, neither of

* Corresponding author. Tel.: +1-412-268-3177; fax: +1-412-268-1513.

E-mail address: rollett@andrew.cmu.edu (A.D. Rollett).

0927-0256/01/$ - see front matter
PII: S0927-0256(00)00216-0

which is fully understood, illustrates the importance of being able to model the recrystallization process in considerable detail. Indeed, since the microstructural evolution process inherent in recrystallization depends on the grain boundary properties which are sensitive to their crystallographic character then the importance of simulation techniques that can model the full range of boundary behavior is apparent.

Computer simulation of grain growth and recrystallization was strongly stimulated in the early 1980s by the realization that MC models could be applied to problems of grain structure evolution. By extension of the Ising model for domain modeling of magnetic domains to the Potts model, it was then possible to represent grains (domains) by regions of similarly oriented (lattice) points [1]. The models have been used, for example, to investigate texture evolution during grain growth and recrystallization, reinforced by parallel work on analytical models [2,3]. A critical issue addressed by Humphreys and others [4–8] extension of grain growth theory is that of coarsening of subgrain networks in order to clarify under what circumstances one expects to observe nucleation of recrystallization. This view of nucleation as simply non-uniform coarsening (i.e., abnormal subgrain growth) is significant for its blurring of the distinction between continuous and discontinuous recrystallization, at least for pure metals in which recovery is rapid.

There are a number of current methods of mesoscopic simulation for recrystallization. The geometrical, method addresses primarily the final microstructural state; it can be used to investigate microstructural evolution, provided that one is not concerned the effect of grain growth occurring in parallel. Such models of recrystallization were first elaborated by Mahin and Hanson [9] and then, developed further by Frost and Thompson [10]. Furu [11] and Juul Jensen [12] have recently extended these models to predict grain size and texture development during recrystallization.

The second method, based on network models, is an efficient way to represent microstructural evolution in discretized form [13–15]. These models are efficient because they abstract a key feature of the grain structure, i.e., the vertices or triple junctions between grain boundaries, and are therefore, efficient because only the vertex motion need be calculated, provided that local equilibrium can be assumed at triple junctions. They have some limitations when second phases must be considered, however, see also the work of Frost [16]. Humphreys [13] has applied the network model to the nucleation process in recrystallization by considering coarsening processes in subgrain networks and also in cases where second phase particles are present [17].

The CA and MC methods discretize the microstructure on a regular grid. Both methods have been successfully applied to recrystallization and solidification. The CA method uses physically based rules to determine the propagation rate of a transformation (e.g., recrystallization, solidification) from one cell to a neighbor [18–21]. The MC method as derived from the Potts model (i.e., a multistate Ising model), has been applied to a wide variety of problems in recrystallization [22–24]. The kinetic MC model simulates boundary motion via an energy minimization procedure for determining a reorientation probability at each step. Other methods that are suitable for recrystallization simulation include the phase-field model [25] and the finite element method [20,21].

3. Current status: limitations of the MC and CA models

Neither the MC model nor the CA model in their standard form is entirely satisfactory for studying boundary migration under the combined influence of two different driving forces. In grain growth, the driving force derives from the curvature of a boundary, [26] for which the MC model is satisfactory. In primary recrystallization, the driving force is the removal of stored dislocations by the migration of the recrystallization front, for which the CA model is satisfactory. In both cases, we expect to find a linear relationship between driving force and migration rate (velocity). The actual behavior of the MC model does not give this for stored energy as a driving force (except for low driving force, see below), however, and the CA

model does not allow for boundary curvature as a driving force.

In the case of the grain growth model implemented in the MC model, one writes a Hamiltonian for the system energy, E,

$$E = \frac{1}{2}\sum_{i}^{n}\sum_{j}^{\mathrm{NN}} J(S_i S_j)(1-\delta_{S_i S_j}), \tag{1}$$

where the inner sum is taken over the NN nearest neighbors of site i (typically first and second nearest neighbors), δ is the Kronecker delta function, and J is the energy of a unit of boundary between elements of indices S_i and S_j. To evolve the structure, a site and a new index are chosen at random. The element is reoriented to the new index with probability, P_{MC}, dependent on the change in energy, ΔE, and the local properties of the boundary.

$$P_{\mathrm{MC}}(S_i, S_j, \Delta E, T) = \begin{cases} \dfrac{J(S_i,S_j)}{J_{\max}}\dfrac{M(S_i,S_j)}{M_{\max}}, & \Delta E \leqslant 0, \\ \dfrac{J(S_i,S_j)}{J_{\max}}\dfrac{M(S_i,S_j)}{M_{\max}}\exp(-\Delta E/kT), & \Delta E > 0, \end{cases} \tag{2}$$

where ΔE is the energy change for the reorientation attempt, including both configurational and stored energy contributions (see Eq. (3), below), M is the boundary mobility between elements of indices S_i and S_j, $J_{\max}$ and $M_{\max}$ are the maximum boundary energy and mobility, respectively, k is the Boltzmann constant, and T is the lattice temperature. After each reorientation attempt, the time is incremented by $1/n$ Monte Carlo Steps (MCS), and a new reorientation is attempted. For a material with uniform boundary energy, the unit boundary energy plays no role in determining the transition probability. Only if a range of boundary energies and/or mobilities is present in the system is the transition probability decreased from the reference value.

It is instructive to plot the transition probabilities at zero temperature, Fig. 1, to illustrate that the transition probability remains at one for zero energy change. Discrete values of the energy change are shown, based on a triangular lattice

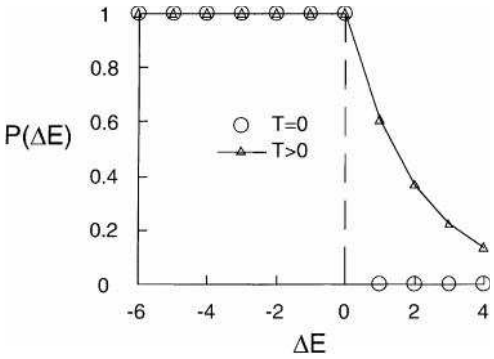

Fig. 1. Plot of transition probabilities for the Potts model as a function of the energy change: note the unit probability for zero energy change. The energy axis is in units of the interaction strength (J) nominally for a triangular lattice in which the maximum change is $\pm 6J$.

and $J = 1$. This feature is critical to the grain growth model because it means that kinks or steps on the boundaries can execute random walks along the boundaries. This, in effect, allows changes in curvature to be communicated along a boundary [27]. Modification of the transition probability from the reference condition decreases the probability linearly with either boundary energy and/or mobility [5].

The MC model has been used extensively to model recrystallization in which case a stored energy term, H_i, is added to the Hamiltonian.

$$E = \frac{1}{2}\sum_{i}^{n}\sum_{j}^{\mathrm{NN}} J(S_i S_j)(1-\delta_{S_i S_j}) + \sum_{i} H_i. \tag{3}$$

At low stored energies, $H < J$, and finite lattice temperature, a linear relationship between migration rate and driving force is recovered. The migration rate of a recrystallization front will be proportional (in the absence of a net curvature) to the difference in forward and backward reorientation rates. That is to say, for sites where the only change in energy is associated with removing or adding stored energy, the migration rate, v, is given by the following, where $J = 1$, $M = 1$, and $H \ll J$.

$$v \propto P_{\mathrm{forward}} - P_{\mathrm{backward}} = 1 - \exp\left\{-\frac{H}{T}\right\} \approx \frac{H}{T}. \tag{4}$$

The structure of a CA model is geometrically very similar with either a triangular or square lattice in two dimensions and either nearest neighbors included in the environment (NN, or von Neumann neighboring), or also next nearest neighbors (NNN, or Moore neighboring). For simulation of recrystallization, the switching rule is simple: any unrecrystallized cell (site) that has a recrystallized neighbor cell will switch to the orientation of that neighbor. Scaling of boundary migration rates is then achieved by relating the ratio of the unit distance (lattice repeat) in the model to the unit time step (maximum velocity in the model) to a maximum migration rate for the specified experiment. Note that the environment of orientations around the site to be reoriented does not affect the outcome of the individual reorientation step. Also if a range of mobilities is present in the system and/or a range of driving forces, then the transition probability is scaled according to a maximum value, following [20,21].

$$P = \frac{M(S_i, S_j)}{M_{\max}} \frac{\Delta H(S_i, S_j)}{\Delta H_{\max}}, \tag{5}$$

where P is the switching probability, M is a mobility that depends on the local boundary character and ΔH is the driving force (spatially variable) which is the difference in stored energy between site i and site j. Raabe also introduces an upper limit on the switching probability that scales with the number of trials such that the smaller the statistical variance desired, the lower the upper limit for the switching probability. The difference between conventional CA and the probabilistic CA models currently used is that in the latter approach: (a) sites are reoriented sequentially; (b) the location of the site to be reoriented is chosen at random; (c) any given reorientation step compares the transition probability to the output of a random number generator (over the interval 0–1) in order to determine whether or not that particular step is successful. Fig. 2 illustrates the variation in probability with magnitude of the change in energy associated with a given change in orientation, with the maximum probability set at unity. This allows for a linear scaling in boundary migration rate with driving force. Note, however, that no reorientation can occur if the energy change is zero or positive in contrast to the MC model.

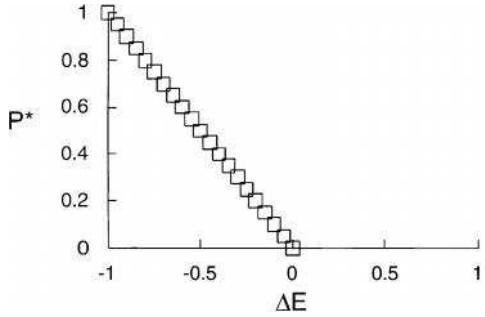

Fig. 2. Plot of the variation in switching probability in the CA model with a range of driving forces or mobilities present, each of which is scaled by a maximum value. Note that the probability goes to zero at zero change in energy.

Again, it is important to note that the framework of the CA model can be adapted to model curvature-driven grain growth provided that a probabilistic local rule is used that reproduces the switching probabilities of the MC model. Even the simultaneous updating of all sites inherent in the CA model can be accommodated by defining sublattices and performing updates on each sublattice in turn (see for example [28, p. 296]). A square lattice requires two sublattices, a triangular lattice requires three, a square lattice with Moore neighboring requires four, and so on. The principle for construction of the sublattices is that, all the neighbors of a site must belong to a different sublattice than that of the site itself. The issue remains of how to write a rule for reorientation that correctly combines both curvature and stored energy as driving forces for boundary motion. This point can be illustrated by attempting to write a switching probability for the combined effect of curvature and stored energy driving forces in order to obtain a linear relationship between migration rate and driving pressure. Based on the particular form presented here, Eq. (6a), the switching probability yields the desired limiting behavior if the grain boundary energy approaches zero, but does not if the stored energy approaches zero because energy neutral switches would have zero probability.

$$P(S_i,S_j,\Delta E,T) = \begin{cases} \left|\dfrac{\Delta E(S_i,S_j)}{\Delta E_{\max}}\right| \dfrac{J(S_i,S_j)}{J_{\max}} \dfrac{M(S_i,S_j)}{M_{\max}}, & \Delta E \leqslant 0, \\ \left|\dfrac{\Delta E(S_i,S_j)}{\Delta E_{\max}}\right| \dfrac{J(S_i,S_j)}{J_{\max}} \dfrac{M(S_i,S_j)}{M_{\max}} \exp(-\Delta E/kT), & \Delta E > 0. \end{cases} \tag{6a}$$

The alternative to this switching probability is to write an additive combination of the curvature and stored energies as follows, where it is understood that ΔE and J are dependent on the local boundary properties and local variations in stored energy.

$$P(S_i,S_j,\Delta E,T) = \begin{cases} \left|\dfrac{(\Delta E+J)}{(\Delta E+J)_{\max}}\right| \dfrac{M(S_i,S_j)}{M_{\max}}, & \Delta E \leqslant 0, \\ \left|\dfrac{(\Delta E+J)}{(\Delta E+J)_{\max}}\right| \dfrac{M(S_i,S_j)}{M_{\max}} \exp(-\Delta E/kT), & \Delta E > 0. \end{cases} \tag{6b}$$

This approach, however, suffers from the defect that the switching probability is not proportional to the change in stored energy as the latter approaches zero because the prefactor is dominated by the grain boundary energy term (J). In an effort to overcome the difficulties of combining the two types of driving force in a single switching probability model, a different approach has been taken.

4. Hybrid algorithm

The new algorithm described here adopts both types of evolution and combines them in a single *hybrid model*. The essence of the hybrid model is to interleave the two different types of reorientation in time. Each sub-model obeys the appropriate rules so that the correct limiting behavior is obtained in the limit that the frequency of either type approaches zero. Such a combination of switching rules has been used to model, e.g., ferromagnetic fluids [29] where it is useful to use spins can move according to a lattice gas model but spin interactions are governed by an Ising model, see p.293 et seq. [28]. A ratio, Γ, between the frequency of CA and MC reorientation attempts determines the relative magnitudes of the grain boundary energy compared with the stored energy. The MC reorientations are determined only by configurational energy such that only the first term on the RHS of Eq. (1) is used to determine ΔE. The effect of stored energy is incorporated into the CA model. For any given reorientation attempt, the choice of which type to apply is governed by a random number, R on the interval $(0,1)$: if the value of R is less than $\Gamma/1+\Gamma$, a CA reorientation is attempted, otherwise an MC reorientation attempt is made. The crucial advantage of this algorithm is that the motion of kinks on boundaries under energy-neutral changes in orientation is preserved which allows curvature driven motion to be modeled: the proportionality of the migration rate of a boundary to the stored energy difference across the boundary is also correctly modeled. Note that in the conventional MC model applied to recrystallization, [22], any energy change less than zero results in the same uniform switching probability (barring local variations in mobility). Therefore, variations in stored energy do not lead to any appreciable variation in boundary migration rate, although they do affect whether or not nucleation can occur homogeneously or heterogeneously [22,30].

5. Gibbs–Thomson

A useful test of the hybrid model is to investigate the behavior of an isolated (island) grain under the combined effects of curvature and stored energy driving forces. When only curvature is present, the grain will shrink by migration of all boundary segments towards their center(s) of curvature, i.e., the center of the grain. The curvature is inversely proportional to the radius and so the boundary velocity accelerates with time, leading to a characteristic constant rate of decrease of area, A, with time [31]. If the effect of a stored energy difference, ΔH, (higher stored energy outside the grain) is included, then $\mathrm{d}A/\mathrm{d}t$ is as follows, where M is a mobility as before, γ is the grain boundary energy and R is the radius of the 2D island grain.

$$\frac{dA}{dt} = -2\pi M\gamma + 2\pi RM\Delta H. \quad (7)$$

Thus, if the grain boundary energy is small and the stored energy difference is large, the grain will grow. For a linear velocity-force relation, one expects to observe a constant velocity, $v = M\Delta p$, and therefore, an accelerating (parabolic) rate of change of area. Furthermore, there should be a balance between the two forces at a critical size given by $\Delta H = \gamma/R_{\text{crit.}}$ ($\Delta H = \gamma/2R$ in the standard, 3D case).

In this hybrid kinetic MC model, the critical size can be estimated as follows for the smallest possible grain of size equal to a single site. Such a grain is surrounded by neighbors of a different orientation such that a fraction $1/Q$ MC reorientation attempts will result in absorption of the unit-size grain into one of its neighbors. If the grain is strain-free but all its neighbors have stored energy i.e., are unrecrystallized then any CA reorientation attempt will succeed in adding another site to the unit-size grain. Subsequent CA reorientations will continue to add more sites to the grain so that it continues to grow. This suggests that, in the limit where the critical grain size for recrystallization is that of unit-size grains, the reorientation frequency ratio is approximately $\Gamma = 1/Q = 0.01$. At larger sizes, however, the ratio should be larger. The analogous equation to Eq. (7) is therefore, the following, where α is effectively the product of mobility and grain boundary energy (in the MC model), μ is the mobility of a boundary in the CA model and Γ is the reorientation ratio. The mobility, μ, is not a free parameter but is determined by the characteristics of the particular form of MC model and CA model chosen.

$$\frac{dA}{dt} = -2\pi\alpha + 2\pi R\mu\Gamma. \quad (8)$$

Fig. 3 shows the area vs time for a single grain of initial radius $20a$ for various choices of the ratio, Γ, between MC and CA reorientations. The simulations were performed on a 50×50 square lattice with first and second nearest neighbors. Note that for ratios close to the critical value any fluctuation of the size will render the grain either super- or sub-critical leading to either growth or shrinkage. The results show the expected parabolic accelerating growth when stored energy dominates and linear shrinkage when curvature driving force dominates.

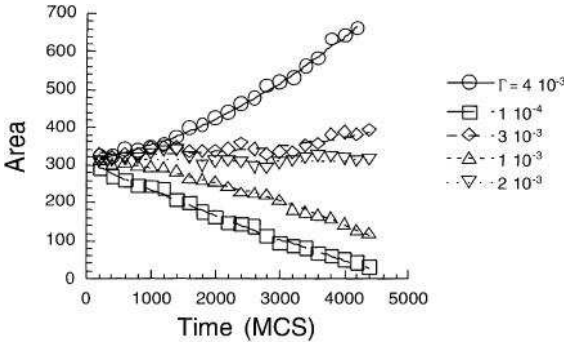

Fig. 3. Plot of area of single grain vs time for various ratios of reorientation frequencies, showing (linear) shrinkage for curvature dominated migration and (parabolic) expansion for stored energy migration. Each set of points has been fitted to a second order polynomial for the purposes of extracting the rate of change of area.

The critical size above which a new grain is stable ($dA/dt > 0$) can be estimated as follows. A single grain shrinking under curvature driven migration does so at a constant rate of change (loss) of area [1]. The magnitude of the rate is dependent on the value of Q because of the definition of the time step in the classical MC scheme. For $Q = 100$ used here and a square lattice, the rate is approximately $-0.1\ a^2\,\text{MCS}^{-1}$, where a is the size of each cell and 1 MCS represents one reorientation step for each cell. Choosing the grain boundary energy to be one sets the mobility, $\alpha = 0.016$. The expected boundary migration rate under stored energy driving force, however, should be approximately one cell per time step, i.e., $\mu = 1$. Therefore, for an isolated grain of size one, the reorientation ratio should be of order $\Gamma = 0.04$ for the curvature and stored energy driving forces to be in equilibrium. Testing the hybrid model at this resolution is impractical of course because statistical fluctuations will obscure the result of interest. Therefore, it is more useful to examine larger initial sizes.

Fig. 3 shows the variation in area with time of an island grain of size $R_0 = 20$ for various stored energies as expressed by the reorientation attempt

ratio. Small values of Γ allow the grain to shrink at a constant rate whereas large values lead to parabolic growth. At intermediate values, the grain is quasi-stationary although any fluctuation away from the zero growth size will lead to either continuing shrinkage or growth. In other words, the zero growth size is a metastable size. For this particular choice of initial grain size, zero growth occurs for $\Gamma \sim 0.002$. By setting $\mathrm{d}A/\mathrm{d}t = 0$ in Eq. (8), this leads to an estimate of the mobility of $\mu \sim 0.4$, which is not too far from unity, as expected. By differentiating the time dependence of the area one can obtain initial rates of change of area. Fig. 4 plots the slope of the area vs time at zero time for three different initial grain sizes and reorientation ratios between 0 and 0.01 with several trials for each set of parameter values. The results show some scatter in the growth rate but the growth rate appears to be linearly dependent on the reorientation ratio.

The relation for the rate of area change above predicts a linear dependence on initial radius with a constant intercept corresponding to a fixed shrinkage rate under the influence of curvature-driven migration only. Eq. (8) suggests that the contributions to the growth or shrinkage rate should all scale by the initial size (at $t = 0$). Fig. 5 therefore, presents the results of scaling the reorientation ratio, $\Gamma_{\mathrm{scaled}} = \Gamma R_0/20$, for the results

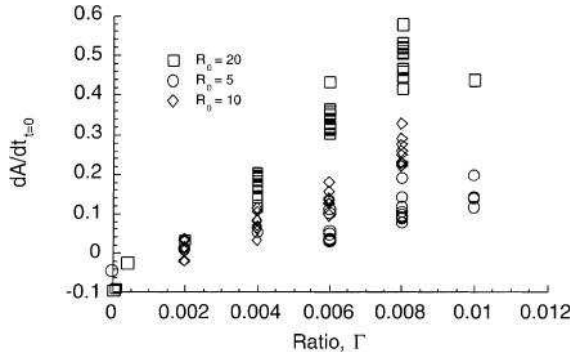

Fig. 4. Plot of initial rate of change of area of an island grain vs the reorientation frequency ratio for three different initials sizes. The larger the initial size of the grain, R_0, the smaller the stored energy required to allow the grain to grow. The predicted variation is approximately linear with stored energy and the ratio (stored energy) corresponding to zero growth is linear in the initial radius.

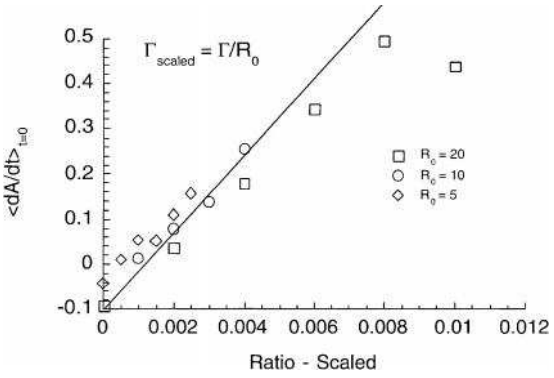

Fig. 5. Initial rate of change of area of an island grain for three different initial sizes, R_0. Each point represents the average for a set of simulations under the same conditions (as shown in Fig. 4). The reorientation ratio has been scaled, $\Gamma' = \Gamma \cdot R_0/20$, in accordance with Eq. (5).

shown in Fig. 4; each point represents an average of the set of trials for a given initial size and reorientation ratio. All the points lie close to a single straight line as expected although the trend is sublinear for large reorientation ratios.

Again, it is important to note that the concept of a critical grain size is not new in this context. Although it is not applicable to the standard form of the CA model as typically used to simulate recrystallization, a critical size can be readily defined in the standard form of the MC model as applied to recrystallization model. Holm [32] has investigated the range of critical sizes for various lattices as follows. Note that the focus is on minimum size required for an embryonic grain to survive and grow into a new grain. Also, certain sizes and shapes of embryonic grains have special properties owing to anisotropy of the lattice. A similar exploration of the behavior standard MC model for recrystallization for critical sizes could be performed. For small values of H/J and with finite lattice temperature, similar results may well be obtained (Table 1).

6. Recrystallization kinetics

In order to verify that the new hybrid model simulates primary recrystallization correctly, the

Table 1
Critical embryo sizes in the standard MC model for recrystallization (Eq. (3)) [32]

Stored energy: boundary energy	Critical size (lattice sites)
2D, triangular lattice	
$H/J < 2$	(very large)
$2 < H/J < 4$	2
$4 < H/J < 6$	1
$H/J > 6$	(any embryo grows)
2D, square lattice, with second nearest neighbors	
$H/J < 1$	(very large)
$1 < H/J < 2$	3
$2 < H/J < 8$	1
$H/J > 8$	(any embryo grows)
3D, simple cubic lattice, with second and third nearest neighbors	
$H/J < 3$	(very large)
$3 < H/J < 5$	5
$5 < H/J < 8$	3
$8 < H/J < 26$	1
$H/J > 26$	(any embryo grows)

behavior of a 2D system was modeled on a 100×100 square lattice with first and second nearest neighbors as before. The reorientation ratio, Γ, was varied and also the number of new grains. The model was operated in normal grain growth until a time of 1000 MCS had been accumulated and then, the recrystallization simulation was started by inserting new grains into the system. The resulting microstructures, Fig. 6, show the anticipated growth of new grains into a polycrystalline matrix that is also undergoing grain growth. The area fraction recrystallized was plotted in the usual double logarithmic plot, Fig. 7, for two values of Γ and three different densities of (site

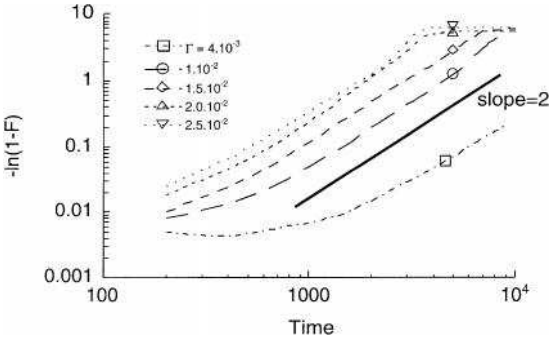

Fig. 7. JMAK plot of fraction recrystallized vs time for site saturated nucleation with 20 embryos and a range of reorientation ratios. Recrystallization proceeds less rapidly for smaller reorientation ratios, i.e., lower stored energy. The slope of the curves approaches two which is the classical value for spatially random, site saturated nucleation and two dimensional growth.

saturated) embryos. The results indicate that the expected Kolmogorov–Johnson–Mehl–Avrami kinetics for 2D growth under site-saturated nucleation conditions are followed, Eq. (9). That is to say, after an initial transient, a slope of two ($=n$) is observed for plots of $\log(\ln(1-F))$ vs $\log(\text{time})$. The time for the preliminary grain growth stage has been subtracted from the total time. Since each embryonic grain is inserted into the microstructure with nine sites, i.e., a central site and its nearest neighbors, not all new grains survived. The disappearance of some new grains gives rise to a transient at short times, particularly for the smallest value of Γ. This aspect of the results suggests that the prior grain structure played a role by supporting heterogeneous nucleation [30].

$$1 - F = \exp -\{kt^n\}. \tag{9}$$

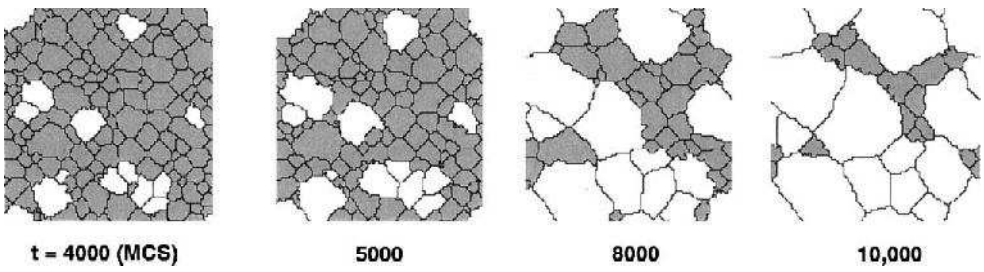

Fig. 6. Microstructural evolution during recrystallization for site saturated nucleation with 20 embryos and $\Gamma = 4 \times 10^{-3}$.

7. Scaling relationships

It is useful to examine scaling relationships between quantities such as time and length in the simulations and their corresponding physical quantities. This is most easily accomplished by considering parallel expressions for the same characteristic quantity. For length, the logical choice is the critical radius at which a nucleus is stable, i.e., $dA/dt = 0$ in Eq. (7). The physical critical size is given by:

$$R_{\text{crit.}}^{\text{physical}} = \frac{\gamma}{\Delta H}. \tag{10}$$

The corresponding expression for the critical radius in the simulations in terms of the areal shrinkage rate under curvature driven motion, $-2\pi\alpha$, the mobility in the CA model, μ, and the reorientation ratio, Γ, is given by:

$$R_{\text{crit.}}^{\text{model}} = \frac{\alpha}{\mu\Gamma}. \tag{11}$$

Equating the critical radii yields the following expression for scaling lengths.

$$x^{\text{physical}} = \frac{\gamma}{\Delta H}\frac{\mu\Gamma}{\alpha}x^{\text{model}}. \tag{12}$$

Since the quantities α and μ are intrinsic properties of the Monte Carlo and CA models respectively, the independent variable in the model is the reorientation ratio, Γ. For a given material with grain boundary energy, γ, and stored energy, ΔH, the larger the value chosen for Γ, the larger the effective magnification in the model (because of smaller $R_{\text{crit.}}$ in the model), or, alternatively, the lower the spatial resolution of the model.

For velocity scaling, one can consider the migration rate of a boundary under a difference in stored energy. In the physical case, the migration is given by, where M is the boundary mobility.

$$v^{\text{physical}} = M\Delta H. \tag{13}$$

In the model, the velocity is scaled by the fraction of steps that are governed by the CA rule:

$$v^{\text{model}} = \mu\frac{\Gamma}{1+\Gamma}. \tag{14}$$

Again, we can equate velocities to obtain a scaling relationship.

$$v^{\text{physical}} = \frac{M\Delta H}{\mu}\frac{1+\Gamma}{\Gamma}v^{\text{model}}. \tag{15}$$

Time scaling is then obtained as the length:velocity ratio:

$$t^{\text{physical}} = \frac{\text{length}}{\text{velocity}} = \frac{\gamma}{M(\Delta H)^2}\frac{\Gamma^2}{1+\Gamma}t^{\text{model}}. \tag{16}$$

In order to obtain a scaling relationship for time in the simulated recrystallization process for various values of the reorientation ratio, however, it is helpful to consider the KJMA relationship. Thus, consider the time required for 50% recrystallization in the case of site saturated, 2D growth. Rearrangement of the standard form, Eq. (9) above, where I is the nucleation density and G is the growth rate,

$$F = 1 - \exp\{-IG^2t^2\}$$

gives the following expression for $t_{50\%}$

$$t_{50\%}^2 = \ln 0.5/IG^2. \tag{17}$$

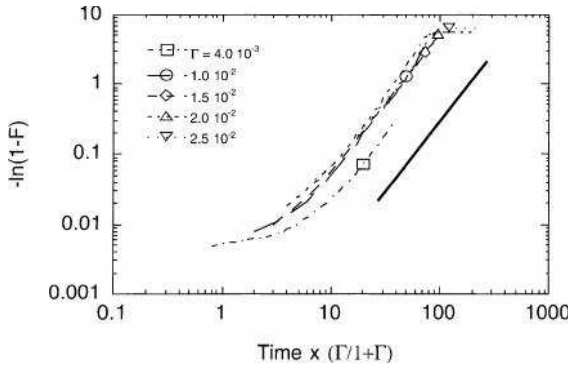

Fig. 8. JMAK plot of the fraction recrystallized vs normalized time according to Eq. (15). All the data follow a master curve describing recrystallization kinetics except for the smallest value of Γ: in this case, the low (effective) stored energy means that a significant fraction of the embryos do not survive to become new grains thereby retarding recrystallization, Eq. (13).

This shows that recrystallization times scale as the boundary velocities, Eq. (15), and not according to the time scaling given in Eq. (16), i.e.,

$$t_{50\%}(\Gamma') = \frac{\Gamma'}{1+\Gamma'}\,\frac{1+\Gamma}{\Gamma}\,t_{50\%}(\Gamma). \tag{18}$$

Fig. 8 shows the same set of data as in Fig. 7 but with the times scaled according to Eq. (18). All the data sets are scaled to the same curve except for the smallest value of Γ, for which not all the embryos survive to become new grains, thereby reducing the effective value of the nucleation density, I, in Eq. (17).

8. Summary

A new approach to mesoscopic simulation of recrystallization has been described that models the Gibbs–Thomson effect correctly. The simulation incorporates two types of reorientation process, one based on curvature-driven migration and one based on stored-energy driving forces. By allowing for two types of reorientation, it is possible to obtain the correct limiting behavior for both types of driving force for migration. The necessity for this arises from the non-local nature of the effect of curvature in the MC model. The kinetics of primary recrystallization for site-saturated conditions are correctly modeled. The hybrid approach can be generalized to three dimensions and should also be applicable to the kinetics and microstructural evolution of phase transformations.

Acknowledgements

Discussions with Professors R. Swendsen, J. Rickman and Drs. E. A. Holm and R. A. LeSar are gratefully acknowledged. This work was supported primarily by the MRSEC Program of the National Science Foundation under Award Number DMR-9632556.

References

[1] M.P. Anderson, D.J. Srolovitz, G.S. Grest, P.S. Sahni, Acta metall. 32 (1984) 783.
[2] G. Abbruzzese, K. Lucke, Acta Met. 34 (1986) 905.
[3] H.J. Bunge, U. Köhler, Scripta metall. et mater. 27 (1992) 1539.
[4] A.D. Rollett, W.W. Mullins, Scripta metall. et mater. 36 (1996) 975.
[5] A.D. Rollett, E.A. Holm, in: T.R. McNelley (Ed.), Proceedings of Recrystallization 96, ReX '96, 1997, p. 31.
[6] F.J. Humphreys, in: T.R. McNelley (Ed.), Proc. Recrystallization-96, ReX'96, 1997, p. 1.
[7] B. Radhakrishnan, G.B. Sarma, T. Zacharia, Scripta mat. 39 (1998) 1639.
[8] F.J. Humphreys, Acta mater. 45 (1997) 4321.
[9] K. Mahin, K. Hanson, J. Morris, Acta Met. 28 (1980) 443.
[10] H. Frost, C. Thompson, Acta Met. 35 (1987) 529.
[11] T. Furu, K. Marthinsen, E. Nes, Mater. Sci. Technol. 6 (1990) 1093.
[12] D. Juul Jensen, Scripta metall. et mater. 27 (1992) 1551.
[13] F.J. Humphreys, Scripta metall. et mater. 27 (1992) 1557.
[14] C. Maurice, F.J. Humphreys, in: H. Weiland, B.L. Adams, A.D. Rollett (Eds.), Proceedings of the Grain Growth in Polycrystalline Materials III, TMS, 1998, p. 81.
[15] V.E. Fradkov, L.S. Shvindlerman, D.G. Udler, Scripta metall. 19 (1985) 1285.
[16] H.J. Frost, C.V. Thompson, D.T. Walton, Acta metall. mater. 40 (1992) 779.
[17] F.J. Humphreys, in: H. Weiland, B.L. Adams, A.D. Rollett (Eds.), Proceedings of the Grain Growth in Polycrystalline Materials III, TMS, 1998, p. 13.
[18] M. Rappaz, C.-A. Gandin, Acta metall. mater. 41 (1993) 345.
[19] H.W. Hesselbarth, I.R. Göbel, Acta metall. 39 (1991) 2135.
[20] D. Raabe, Mater. Sci. Forum 273–275 (1998) 169.
[21] D. Raabe, Phil. Mag. A 79 (1999) 2339.
[22] D.J. Srolovitz, G.S. Grest, M.P. Anderson, Acta metall. 34 (1986) 1833.
[23] A.D. Rollett, D.J. Srolovitz, M.P. Anderson, R.D. Doherty, Acta metall. 40 (1992) 3475.
[24] P. Tavernier, J.A. Szpunar, Acta metall. mater. 39 (1991) 557.
[25] L.-Q. Chen, Scripta metall. et mater. 32 (1995) 115.
[26] C. Herring, Phys. Rev. 82 (1951) 87.
[27] P. Sahni, D. Srolovitz, G. Grest, M. Anderson, S. Safran, Phys. Rev. B 28 (1983) 2705.
[28] B. Chopard, M. Droz, Cellular Automata Modelling of Physical Systems, Cambridge University Press, Cambridge, 1998.
[29] V. Sofonea, Europhys. Lett. 25 (1994) 385.
[30] D.J. Srolovitz, G.S. Grest, M.P. Anderson, A.D. Rollett, Acta metall. 36 (1988) 2115.
[31] W.W. Mullins, J. Appl. Phys. 27 (1956) 900.
[32] E.A. Holm, personal communication, 1996.